



RESEARCH ARTICLE



Conversion of coffee and plastics residues into activated carbon by chemical activation with ammonia

Rodrigo Surculento-Villalobos^{1*} ; Luis Lopez N.¹ 

¹ Universidad Mayor de San Andrés (UMSA), Facultad de Ciencias Puras y Naturales (FCPN), Instituto de Investigaciones Químicas (IIQ), Campus Universitario Calle 27 de Cota Cota, La Paz, Bolivia.

* Corresponding author: rsurculento31@gmail.com (R. Surculento-Villalobos).

Received: 3 December 2025. Accepted: 9 March 2026. Published: 7 April 2026.

Abstract

Aiming for the valorization of agricultural biomass residues such as coffee husks and plastics wastes such as polyethylene terephthalate (PET), a method for transforming them into activated carbon by using ammonia chloride as activation agent is presented in this study. Firstly, mixtures of PET waste were processed through a pyrolytic process at different operational conditions through a factorial experimental design. The obtained material with the best characteristics of specific surface area (SSA) and mass yield was obtained at 600 °C and 2.5 hours of treatment. These parameters were then used for performing the activation of coffee husks residues and mixtures of them with PET (in mass rates of 1:1 and 1:2 of PET and biomass, respectively) All the obtained materials were then characterized through a Scanning Electron Microscopy - Energy Dispersive Spectroscopy (SEM-EDS), X-Ray Fluorescence (XRF), X-Ray Diffraction (XRD) and a Differential Scanning Calorimetry - Thermogravimetric Analysis (DSC-TGA) technique, and other physicochemical properties (particle size, bulk density, humidity content and ash content) were also measured, all properties were then compared with characteristics of commercial activated carbon. The activated carbon obtained from coffee husks residues showed a low specific surface area (SSA) and a higher pyrolysis yield. The mixtures of biomass and PET showed lower SSA and higher pyrolysis yield than the ones obtained from PET. The mixture of 1:1 is the best on SSA and yield. The textural analysis was performed (BET, BJH, XRF, XRD and SEM-EDS) on the samples of pure pet and mixture 1:1. This shows that the method allows the utilization of coffee and PET residues to produce activated carbon in a more sustainable way respect to other methods of activation (the proposed method uses low mass relations 10% and no postprocessing). This material was then tested for CO₂ removal determining the adsorption isotherm model and the kinetic parameters of sample 1:1 and activated carbon from PET.

Keywords: Activated carbon; pyrolysis; biomass residues; plastic waste.

DOI: <https://doi.org/10.17268/sci.agropecu.2026.029>

Cite this article:

Surculento-Villalobos, R., & Lopez, N. L. (2026). Conversion of coffee and plastics residues into activated carbon by chemical activation with ammonia. *Scientia Agropecuaria*, 17(2), 409-418.

1. Introduction

Biomass and plastic residues treatment represent an important environmental and economic challenge for the world. Biomass residues are normally derived from agricultural activities (in the case of this study; coffee husks), these often pollute producing communities. On the other hand, plastic waste, in particular Polyethylene terephthalate (PET), is a major issue since they accumulate in landfills and in water bodies due to its slow degradation. For this study coffee husks residues from one of the Bolivia's main producing regions (Caranavi, La Paz) are going to be processed for activated carbon production in mixture with PET residues. The inadequate management of these residues causes several issues such as air and water

pollution, land scarcity for disposal and accumulation and pest proliferation.

To address these issues, this study aims to propose a process of valorization of mixtures of Coffee Husks and PET wastes, this will be achieved through the design of a pyrolytic process. Pyrolysis is a thermochemical process that uses heat to induce thermal degradation of a material into valuable products such as biochar, activated carbon, bio-oil, and syngas. Activated carbon is a porous material commonly used on water purification, gas adsorption and other chemical applications. Pyrolysis is interesting for this purpose because of its versatility which allows the obtention of high-quality solids, liquids and gases (Block et al., 2019; Paradelo et al., 2009; Scheirs & Kaminsky, 2006).

Pyrolysis of PET is normally a process that is not commonly used for activated carbon generation but focuses more on the liquid and gas compounds of the process, however, there is some previous work on this subject (Surculento Villalobos et al., 2023). In contrast, this study focuses on the generation of AC from PET residues enhancing the SSA of the material and then study the co-processing with coffee husks.

Coffee husks transformation into biochar is a field that has been studied widely (Guimarães et al., 2020) however, the activation process of this residue has been studied less (Ciner et al., 2026; Ramirez et al., 2020), it is important mentioning that there are different methods of activation and different activation agents (KOH, H₃PO₄, ZnCl, etc.) (Cai et al., 2026; Newar et al., 2026; Nguyen et al., 2026; Serafin, 2017) in our case we intend to evaluate how good NH₄Cl performs when activating PET residues by using a two stage activation (López Nina et al., 2021; Moussavi et al., 2013).

The proposed pyrolytic process is composed by two stages, the first one consists in a traditional pyrolysis of the material at low temperatures to ensure carbon fixation on the solid material (PET at first for the experimental design and then study the mixtures) and the second is the chemical activation process induced by pyrolysis as seen in (Illingworth et al., 2022; Şahin et al., 2016).

The experimental part of this study involves determining the optimal pyrolysis operational conditions for PET, followed by processing coffee husks and PET – coffee husks residues mixtures by using a factorial experimental design 2² with three replicates, considering as factors processing temperature and processing time. Activation agent dosage has been studied previously (López Nina et al., 2021; Moussavi et al., 2013) and therefore will be fixed for this study.

About the CO₂ removal evaluation, there are several studies on the performance of biochar and activated carbon from different biomass feedstocks including coffee husks (Ciner et al., 2026; Ramirez et al., 2020; Serafin et al., 2018) however, fewer studies have been performed on plastic residues and mixtures of both.

Respect to the CO₂ removal textural analysis, adsorption isotherm determination and kinetics of the adsorption are parameters commonly determined to assess the performance of the material for activated carbon and application (Rajadurai & Chandradass, 2024; Serafin & Dziejarski, 2023).

Considering all the above, this study aims to process coffee husks residues, PET residues and their mixtures into activated carbon through a two

stages pyrolytic process optimized with an experimental design, then characterize the material to compare the quality of the obtained products with characteristics of commercial activated carbon finally evaluate the material performance on CO₂ removal.

By transforming these residues into a value – added product, this study tries to generate a sustainable option for waste management with NH₄Cl, which has not been applied on PET nor in coffee husks as activating agent.

2. Methodology

2.1 Materials

The biomass residues (coffee husks) were collected in Caranavi - Bolivia. The plastic residues (PET) came from soda and water bottles of different sources with different grades of age. The ammonia chloride used in this study was of analytical grade, CO₂ gas was of 99.999% purity, Helium and Nitrogen gas were of 99.99999% purity.

2.2 Pyrolysis of PET

To determine the temperature of the first pyrolysis, PET was grinded to a particle size of 2 mm and then introduced into a SETARAM 1600 TGA – DSC for the obtention of the thermal degradation curve of the material. According to (Chia et al., 2020), around 20 to 25% of char should be fixed when working between 320 to 400 °C and for 120 minutes, After the adequate temperature was determined from TGA analysis PET residues were introduced into an electric tubular furnace at that temperature in a nitrogen atmosphere for 2 hours.

2.3 Chemical activation

Carbonized PET was impregnated with ammonia chloride at 10% w/w in a solution prepared with distilled water for 24 hours at 60 °C under stirring (Moussavi et al., 2013). The impregnated material was then dried and divided in 12 samples which were then introduced into the electric tubular furnace under nitrogen atmosphere at temperatures and processing times determined by a factorial experimental design 2² (by triplicate) with a temperature range of 450 – 600 °C and with a process time range of 0.5 – 2.5 hours, with 3 replicates and using specific surface area (SSA) and mass yield as responses.

2.4. Specific surface area determination

The determination of SSA was done with ChemBET of Quantachrome by physisorption of nitrogen into the surface of the material and using helium as a reference gas according to ASTM D 6556-14, the method of calculation for the determination of SSA

was the single point BET method. The experimental design was analyzed utilizing an Analysis of Variance (ANOVA) with the software Design Expert 11.

2.5 Coffee husks residues and residues mixtures activation

For the pyrolysis of coffee husks residues, the material was introduced into a tubular electric furnace as done for PET in section 2.2, then the material was impregnated with ammonia chloride at 10% in mass and then activated in a tubular electric furnace as mentioned in the section 2.3, the characterization of this material for SSA and the other parameters but SEM – EDS were made as commanded by 2.4 and 2.5. In the case of the mixtures, two mass rates of mixtures were analyzed, 1:1 and 1:2 of PET and Coffee husk residues respectively. These mixtures were made before the pyrolysis of the material mentioned in 2.2, then the process was the same as mentioned in 2.3, 2.4 (but SEM – EDS) and 2.5.

2.6. Characterization of the materials obtained

The SEM – EDS analysis was performed with an Oxford SEM analyzer. The XRF analysis was made with a Rigaku NEX QC + QuantEZ analyzer. XRD analysis was made using a Rigaku MiniFlex 6G. TGA – DSC analysis was performed with a SETARAM DTA – 1600 utilizing nitrogen as carrier. The determination of particle size was made with ASTM sieves according to ASTM C 136 – 01 and ASTM C117 – 95. Bulk density was determined according to ASTM C 127. Humidity content was determined utilizing a thermogravimetric analyzer according to the norm UNE – EN 14774 – 1. Ash content was determined by a thermogravimetric analyzer according to the norm ISO 11358-1:2014.

2.7. Surface area and mean pore diameter

To determine the specific surface area of the samples on the design the analysis of single point BET was applied and for the optimal material and the mixture with coffee husks the method applied was multipoint BET, also for these samples a BJH with 6 points was performed. All these analyses were performed into a ChemBET Pulsar of Quantachrome using N₂ and He mixtures for the determination through physisorption.

2.8. Adsorption isotherm and kinetics parameters determination of CO₂ removal

For the CO₂ removal parameters determination were performed into a ChemBET Pulsar system of Quantachrome, for this purpose, mixtures of He/CO₂ at different partial pressures (0.05, 0.08, 0.10 and 0.20) were fed to the system, to induce the adsorption and desorption of CO₂, iced water (at 5°C) and hot water (at 80°C) baths were applied on the sample while under a mixed stream. Then the Sips model and the Avrami – Erofeev model (Serafin & Dziejarski, 2023; Shafeeyan et al., 2015) were applied to fit the adsorption isotherm and kinetics data respectively.

3. Results and discussion

3.1 Pyrolysis of PET residues

The thermogram profile obtained for the degradation of PET is shown in **Figure 1**, suggesting that around 400 °C the degradation of PET starts and finishes at around 450 °C. This decomposition profile is similar to the reported in literature (Chia et al., 2020). 47g of PET residues resulted in 9.8 g of char thus a mass yield of 20.95%.

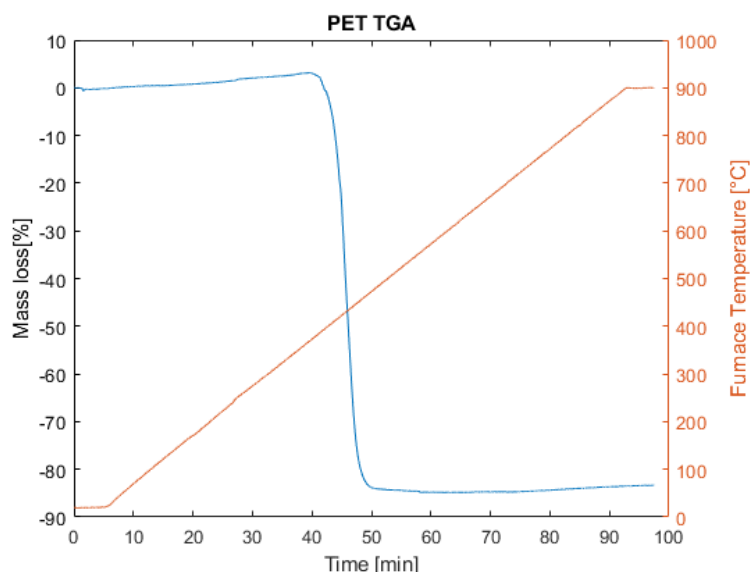


Figure 1. Thermal degradation profile of PET residues.

3.2 Chemical activation

The material obtained after the impregnation with ammonia chloride was processed according to description of the methodology, the results are shown in **Table 1**. The statistical analysis of SSA and mass yield responses by ANOVA is shown in Table that the experimental design showed that for the SSA variable both effects; temperature and time, and their interaction are significant, temperature has a positive effect on the variable and time also increases the SSA.

On the other hand, in the case of mass yield, the ANOVA analysis shows that only Temperature plays a significant role on the process mass yield having a negative effect on the variable. To choose the best activated carbon from the experimental design, the criteria used was the maximization of SSA which made the experiments developed at 600 °C in 2.5 hours the best materials obtained from the design.

3.3 Obtention of activated carbon from coffee husk and PET residues

Coffee husks residues and mixtures with PET at ratios 1:1 and 1:2 were processed into biochar with a pyrolysis at 400 °C and 2 hours according to what was mentioned in section 2.3. To summarize, the results of mass yields of the first pyrolysis are shown in **Table 2**.

Table 2

Mass yield comparison of products from the first pyrolysis step

Sample	1:0	1:1	1:2	0:1
Initial mass [g]	47	61.614	60.408	96.214
Biochar mass [g]	9.849	17.139	17.200	32.590
Yield %	20.95 %	27.81%	28.47%	33.87%

Note: 1:0 refers to pure PET and 0:1 is the sample of pure coffee husks residues.

After this carbonization the coffee husks and mixtures were impregnated and activated at 600 °C and 2.5 hours. The results of this process are shown in **Table 3**. It is important to note that activated carbon from PET was optimized to obtain the

Table 1

Experimental design applied for PET activation

Sample	%NH ₄ Cl	Temperature [°C]	Time [horas]	Initial Mass [g]	Final Mass [g]	Mass yield [%]	SSA [m ² /g]
3	10	600	2.5	1.960	1.417	72.3	441.4
3	10	600	2.5	1.246	0.845	67.8	482
3	10	600	2.5	1.246	0.849	68.1	482.5
4	10	600	0.5	1.918	1.400	73.0	400.5
4	10	600	0.5	1.246	0.834	66.9	378.3
4	10	600	0.5	1.246	0.817	65.6	432.1
1	10	450	2.5	1.960	1.504	76.7	156.5
1	10	450	2.5	1.248	0.909	72.8	167.6
1	10	450	2.5	1.126	0.826	73.4	143.1
2	10	450	0.5	1.960	1.550	79.1	48.5
2	10	450	0.5	1.245	0.941	75.6	35.2
2	10	450	0.5	1.246	0.915	73.4	30.7

highest mass yield possible. Besides, there is a positive tendency while adding coffee husks residues to the mixtures in both pyrolytic processes.

Table 3

Mass yield comparison of products from the activation pyrolysis

Sample	1:0	1:1	1:2	0:1
Initial mass of char [g]	1.246	17.139	17.200	32.590
Activated carbon mass [g]	0.834	13.319	13.241	27.596
Yield %	66.93%	77.71%	76.98%	84.47%

Note: 1:0 refers to pure PET and 0:1 is the sample of pure coffee husks residues.

3.4 Characterization of the materials obtained

X-Ray Fluorescence (XFR)

The analysis of XFR was performed utilizing a method of oxide powders in the equipment as shown in **Table 4**. The raw material was found to have a high concentration of K and Ca, while the other elements were present in trace amounts. Furthermore, the concentration of all compounds decreased after processing, except for Cl. This, combined with the consistent K content, suggests that Cl is bound to the material (and vice versa) by the K. It can be inferred that the compound that is formed is KCl which will be confirmed on XRD analysis. This might be caused by interactions of potassium existing on the biomass with Cl from the activating agent (NH₄Cl).

Table 4

XRF analysis of the activated carbons

Sample	1:0	1:1	1:2	0:1	Feedstock
Cl (%)	0.0043	1.86	1.55	1.6	0.167
Al ₂ O ₃ (%)	3.68	0.28	0.30	-	-
SiO ₂ (%)	4.51	0.14	0.18	0.11	0.352
P ₂ O ₅ (%)	0.02	0.33	0.39	0.39	0.511
SO ₃ (%)	0.03	0.11	0.13	0.20	0.685
K ₂ O (%)	-	2.37	2.03	2.19	10.6
CaO (%)	0.06	0.78	0.82	0.77	4.018

X-Ray Diffraction (XRD)

The XRD analysis was performed for duplicate for PET activated carbon and single reads for 1:1, 1:2 and 1:0. The results obtained from this analysis are shown in **Figure 2**.

The XRD plots of the activated carbon from PET a) and b) show a behavior that according to bibliography follows the conventional shape of activated carbon (Riyanto et al., 2020), this confirms the existence of amorphous carbon structures in the material, on the contrary the activated carbon obtained from the mixtures of PET and coffee husks shows sharp peaks. In the case of c), d) and e), we can see that there is an intense peak on $26^\circ 2\theta$, one of medium intensity at $44^\circ 2\theta$ and a small one around $50^\circ 2\theta$. These peaks were identified KCl, which as mentioned before in the XRF analysis can

be attributed to the interaction of potassium presented prior in the feedstock with the activation agent.

Scanning Electron Microscopy and Energy Dispersive Spectroscopy (SEM - EDS)

SEM analysis showed that there are amorphous structures on the surface of the material, which is an important characteristic of activated carbon. The analysis also showed the existence of meso and macro pores in the surface of the material as shown in Figure 3 and Figure 4.

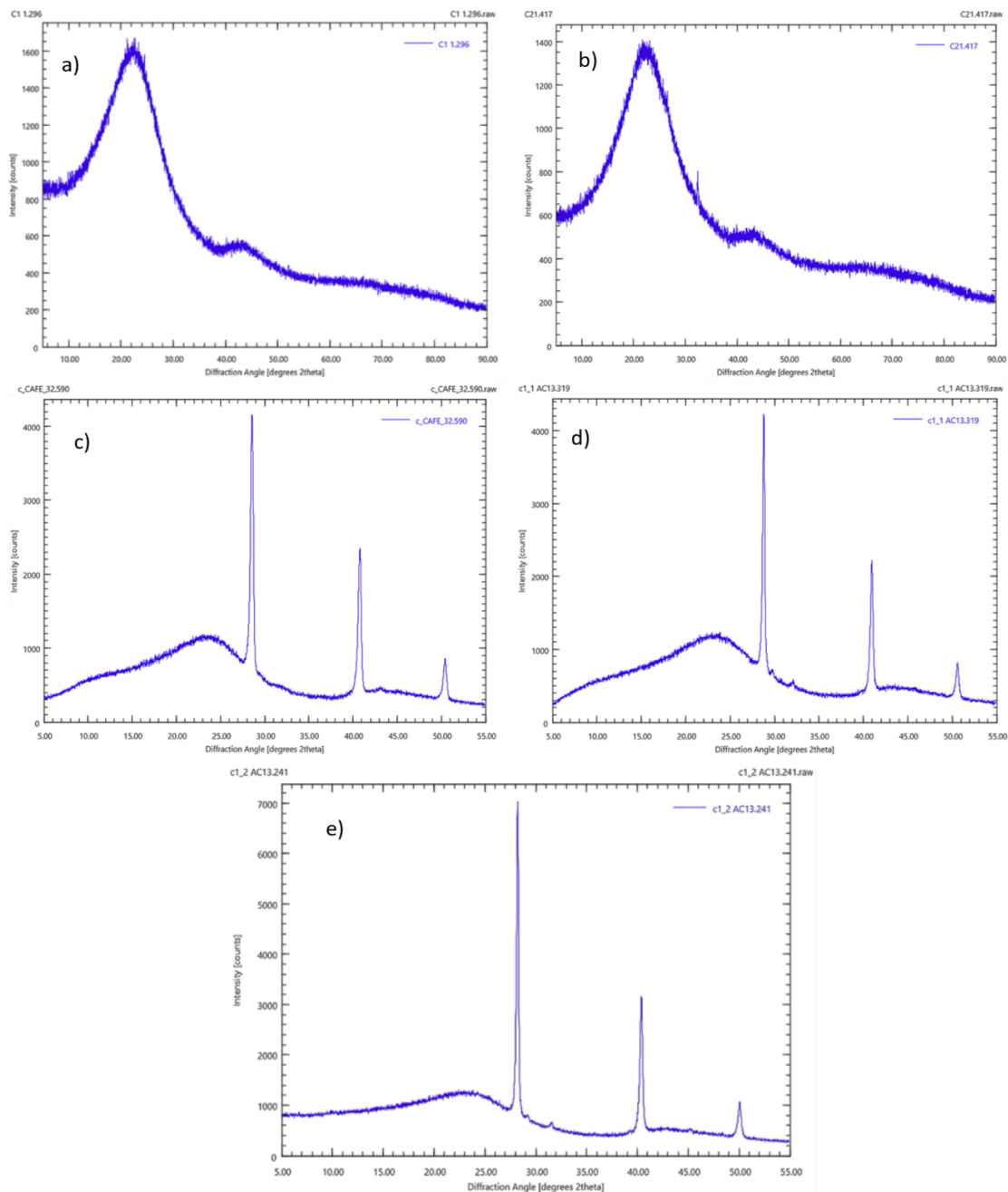


Figure 2. XRD analysis of activated carbons.

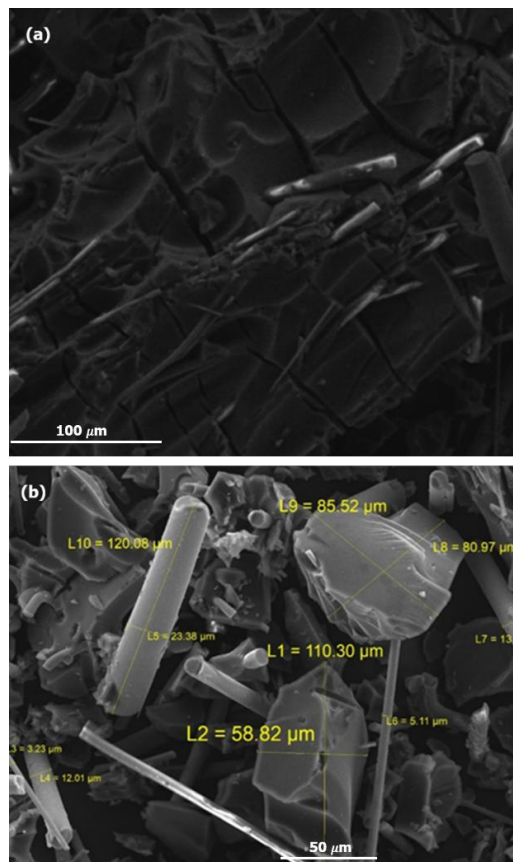


Figure 3. SEM analysis of PET activated carbon: (a) 100 μm , (b) 50 μm .

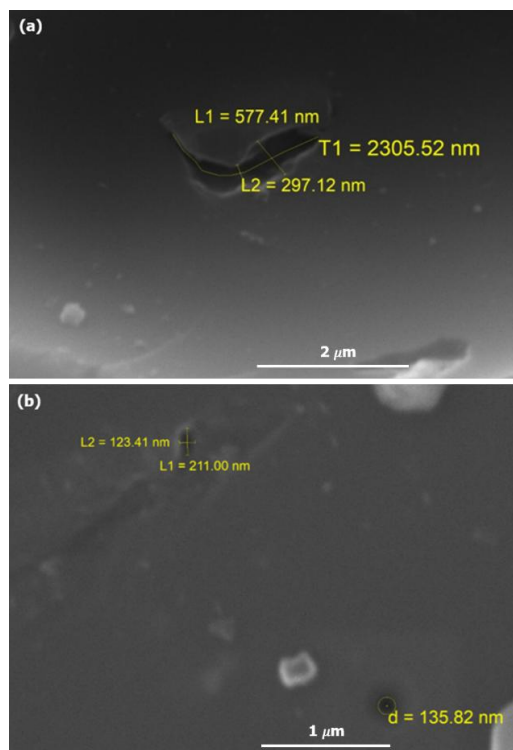


Figure 4. Macro structures found in PET activated carbon: (a) 2 μm , (b) 1 μm .

The EDS analysis of the material shows the existence of oxygenated groups on the surface of the activated carbon, which is expected of this type of material. Also, presence of aluminum and silicium is shown which supports what was found through the XRF analysis, the graphs obtained from this analysis are shown in **Figure 5**. The EDS analysis shows that PET-AC has traces of alumina and silicon. This confirms what the analysis XRF results.

3.5 Surface area and pore diameter

The multipoint analysis of surface area was performed in samples 1:0 and 1:1, the results are shown in **Figure 6**. In addition, a BJH analysis was performed on these samples with 6 points, the results of the plot of pore size distribution are shown in **Figure 7**.

The results that were obtained from these two analyses are summarized in Table 5. The textural analysis shows for the sample 1:0 showed the existence of meso and macropores in the SEM analysis, through the BJH analysis we could determine a mean pore diameter of 9.88nm and a specific surface area of $445.64 \pm 36.86 \text{ m}^2/\text{g}$. the micro pores volume and the total pore volume relation show that there is an approximate of 49% of micropores and the rest are distributed among meso and macropores, confirming what was found in SEM analysis, and for the sample 1:1 shows that there is a 61.8% of micropores, and the left 38.2% are meso and macro pores, these have a mean pore diameter of 9.91 nm and have a specific surface area of $304.54 \pm 19.54 \text{ m}^2/\text{g}$, the material can be qualified as a mixed porosity. From this analysis we can say that the sample 1:0 shows a more equilibrate distribution.

3.6 Physicochemical characteristics and comparisons

The analysis of the other physicochemical characteristics was performed according to the methodology mentioned in last section. To summarize these results **Table 6** shows all parameters that were measured during this study. The material obtained has potential similarities to the range of values of the properties of commercial activated carbon. This shows that successfully a potential material similar to commercial one was obtained from not only pure materials of PET and Coffee husks but also from mixtures. It is important to notice SSA decreases as the coffee fraction increases from $445.64 \text{ m}^2/\text{g}$ with pure PET to $150.25 \text{ m}^2/\text{g}$ in 1:2 sample, in contrast mass yield slowly increases when adding coffee husks to the mixture.

Table 5
Summary of surface area and BJH analysis results

Sample	1:0	1:1
Specific Surface Area [m ² /g]	445.64 ± 36.86	304.54 ± 19.54
Mode Diameter [nm]	9.92	9.92
Mean pore diameter [nm]	9.88	9.91
Micro pores volume [cm ³ /g]	0.037	0.025
Total pore volume [cm ³ /g]	0.076	0.041

Table 6
Summary of the physicochemical characteristics of all activated carbons

Sample	1:0	1:1	1:2	0:1	Commercial material
Specific Surface Area [m ² /g]	445.64	304.54	150.25	54.09	500 – 1500 (MELLIFIQ, 2025)
Mass yield from feedstock to activated carbon [%]	20.96%	21.62%	21.92%	28.68%	25% – 50% (Marsh & Rodríguez-Reinoso, 2006)
Particle size [sieve #]	35	60	60	>18	30 – 40 (Marsh & Rodríguez-Reinoso, 2006)
Bulk density [g/ml]	0.6072±0.0003	0.3265±0.0553	0.2803±0.0276	0.2026±0.0093	0.4 – 0.6 (MELLIFIQ, 2025)
Humidity content [%]	15	0.44	0.98	0.47	1 – 5 (González-García, 2018)
Ash content [%]	4.2	5.9	5.4	5.2	2 – 5 (González-García, 2018)

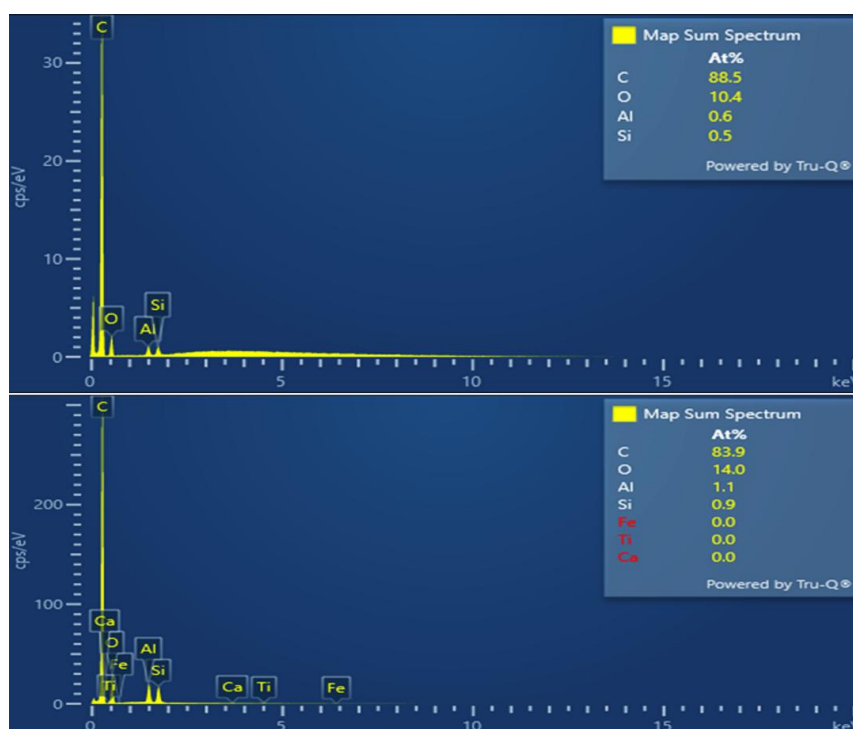


Figure 5. EDS analysis of PET activated carbon.

3.6 Adsorption of CO₂ kinetics and isotherms

As a complementary part of the study, CO₂ removal was tested as a potential application of the material, tests were performed to determine the kinetics and the isotherm of the adsorption of CO₂ on a gas stream. To do this, samples of activated carbon samples 1:0 and 1:1 were tested using a Chembet Pulsar of Quantachrome. Mixtures of CO₂/He were fed to the system at different partial pressures and adsorption, and desorption were induced by using hot and cold baths according to the methodology.

Then, data was adjusted to Sips model.

$$q_e = \frac{q_m * (b * P/P_o)^n}{1 + (b * P/P_o)^n}$$

In this model q_e represents the adsorbate adsorbed at equilibrium (mmol/g), q_m represents the maximum adsorption capacity, b represents the affinity constant and n is the heterogeneity factor. For both materials 1:0 and 1:1 the isotherms are shown in the following figures.

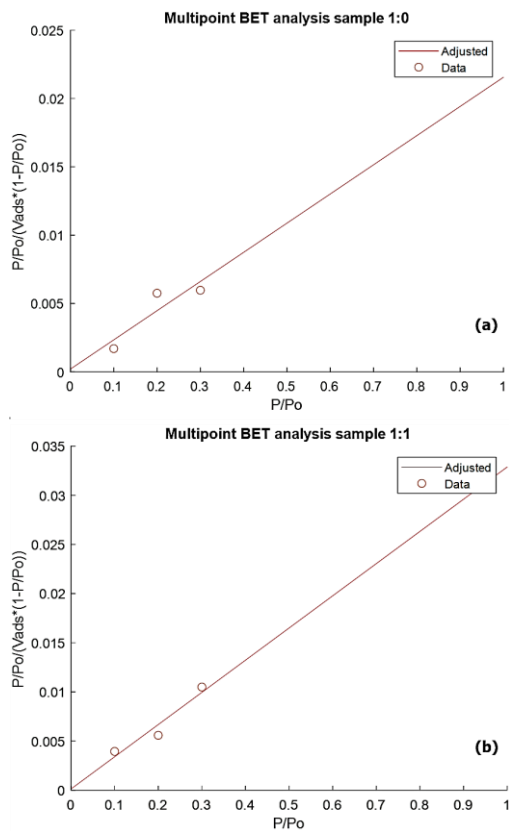


Figure 6. BET analysis of samples 1:0 (a) and 1:1 (b).

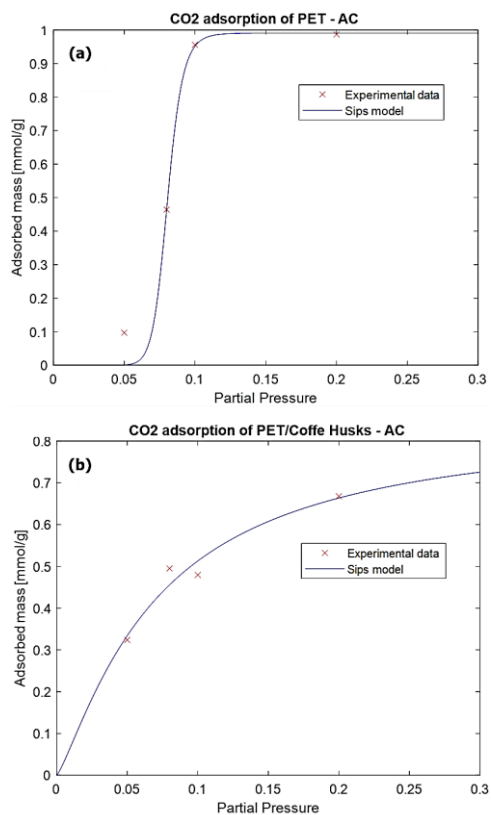


Figure 8. Sips Isotherms of samples 1:0 (a) and 1:1 (b).

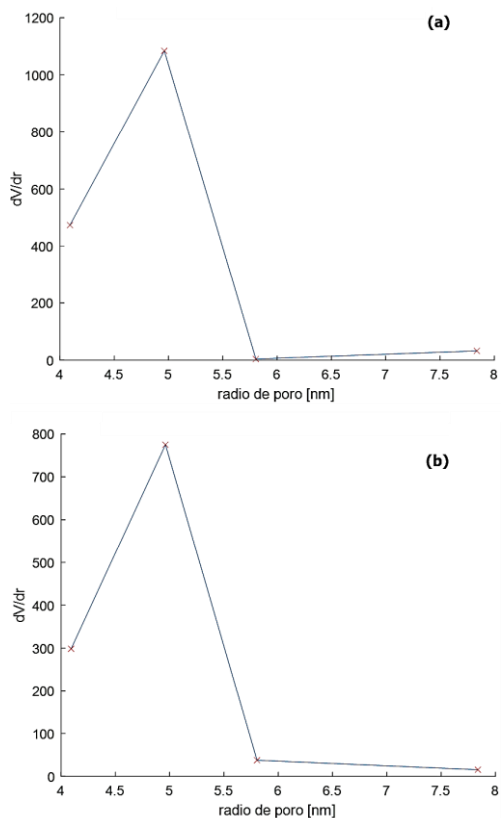


Figure 7. BJH analysis of samples 1:0 (a) and 1:1 (b).

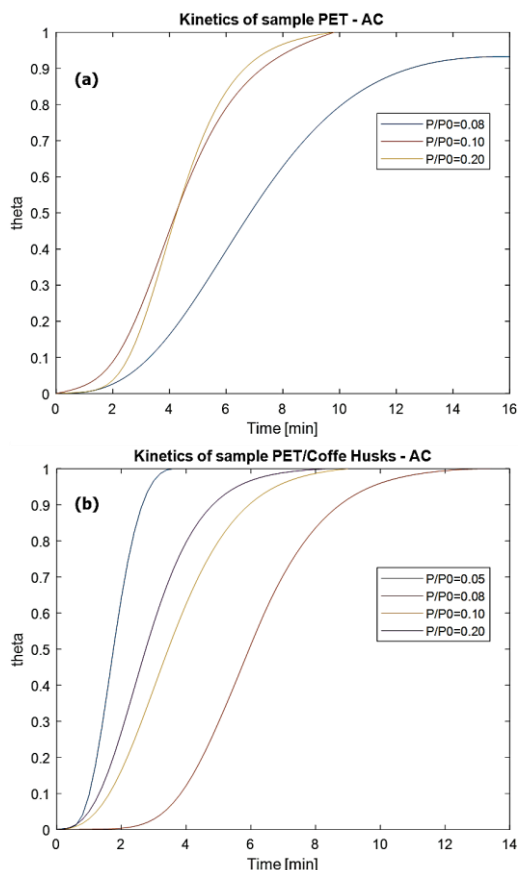


Figure 9. Kinetic behavior of samples 1:0 (a) and 1:1 (b).

The kinetic parameters determined for the Avrami – Erofeev model are shown in the **Table 7**. For these results the following parameters were determined.

Table 7

Sips parameters of samples 1:0 and 1:1

Sample	Q _{max} mmol/g	b	n	R ²
PET – AC 1:0	0.9909	12.3980	0.0674	0.9830
PET/Coffe Husk 1:1	0.8472	14.1357	0.8085	0.9530

The highest maximum adsorption capacity belongs to the sample of PET – AC in comparison to the mixture 1:1, however the affinity is higher in the second sample. This might be related to the presence of KCl confirmed on XRD analysis which according to bibliography enhances the micropores development (Mochizuki et al., 2025). Both materials can be applied for the removal of CO₂ at low pressures as expected of materials of this SSA. For the kinetics study, data was collected and fitted by using the Avrami – Erofeev kinetic model, which is good for describing heterogeneous surfaces. In the figures below, the behavior of $\theta(t)$ will be shown respect to time at different partial pressures.

Table 8

Avrami – Erofeev parameters of samples 1:0 and 1:1

Sample	P/P ₀	K _a [1/min]	m	R ²
PET – AC 1:0	0.08	0.1212	2.1786	0.9960
	0.10	0.1999	2.4081	0.9991
	0.20	0.2042	3.0377	0.9981
PET/Coffe Husk 1:1	0.08	0.1491	3.5578	0.9983
	0.10	0.2451	2.3163	0.9996
	0.20	0.3050	2.2793	0.9993

The results show (**Table 8**) that for 1:0 the values of the rate constant (K_a) and the Avrami exponent (m) have a proportional behavior. From the rate constant we can see that the values increase slowly but Avrami constant incases significantly. This can be seen specially on the change of 0.10 to 0.20 partial pressure where the rate constant gets stuck and the m value rises from 2.41 to 3.04 which can be interpreted as a change from a 2D to a 3D. On the other hand, sample 1:1 has an opposite behavior rate increases as Avrami's constant decreases. The value of m starts at 3.55 and decreases to 2.27 as partial pressure increases from 0.08 to 0.10 while rate constantly increases. This shows a fast capture of CO₂ at low pressures, however, as pressure increases pores saturate, lowering the m value.

4. Conclusions

The results revealed that NH₄Cl is a promising activating agent for PET residues not only because

of the quality of the activated carbons obtained but also for the low amounts of reagent used in the process. Also, the activated carbon obtained from the process does not require further post treatment lowering costs of production respect to other activating agents. The two stages process proved to be effective for the obtention of activated carbon from PET residues only and was then extrapolated for mixed processing with coffee husks. Textural properties of samples were determined and showed that activated carbon from PET is a more balanced material in terms of structure, in contrast when coffee husks are mixed in the process generates a material with more microporous. Then, samples were tested for CO₂ removal where isotherms and kinetics were determined. The mixed sample of PET and coffee husks showed a higher selectivity towards CO₂ with a greater capacity for quick CO₂ removal which was explained by the KCl content formed during the synthesis. Activated carbon from PET showed a more sustained CO₂ removal over time with a larger holding capacity. The addition of coffee husks to PET processing allows the obtention of two activated carbons with different potential usages, reducing surface area and increasing selectivity. It is of high importance that further analysis is performed to complete the isotherms of CO₂ adsorption and the BJH analysis. Other concentrations of NH₄Cl should be considered for next studies. The obtained materials should be tested for removal of other pollutants.

Acknowledgments

This work was supported by the Swedish International Development Cooperation Agency (SIDA) through the 'Producción de Materiales Renovables y Aplicaciones' (PRMA) subprogram of the UMSA – ASDI cooperation program, and by the Erasmus+ Project 'EU – BEGP Modernizing Digital Education in Energy Transition for Circular Economy in Latin America'.

ORCID

R. Surculento-Villalobos  <https://orcid.org/0009-0000-3938-1275>

N. L. Lopez  <https://orcid.org/0000-0001-8488-4429>

References

- Block, C., Ephraim, A., Weiss-Hortala, E., Minh, D. P., Nzihou, A., & Vandecasteele, C. (2019). Co-pyrogasification of Plastics and Biomass, a Review. *Waste and Biomass Valorization*, 10(3), 483–509. <https://doi.org/10.1007/s12649-018-0219-8>
- Cai, X., Ren, W., Li, C., Li, Q., & Hu, X. (2026). Synergistic CO₂-K₂C₂O₄ activation of furfural residue toward high-adsorption activated carbon for phenol removal. *Journal of Analytical and Applied Pyrolysis*, 193, 107408. <https://doi.org/10.1016/j.jaap.2025.107408>
- Chia, J. W. F., Sawai, O., & Nunoura, T. (2020). Reaction pathway of poly(ethylene) terephthalate carbonization: Decomposition behavior based on carbonized product. *Waste Management*, 108, 62–69. <https://doi.org/10.1016/j.wasman.2020.04.035>

- Ciner, M. N., Özbaşı, E. E., Özcan, H. K., & Ongen, A. (2026). Potential of Physical Activated Carbon Derived from Pyrolyzed Waste Coffee Grounds as an Adsorbent for Dye Removal. *Water, Air, and Soil Pollution*, 237(9). <https://doi.org/10.1007/s11270-026-09235-4>
- González-García, P. (2018). Activated carbon from lignocellulosics precursors: A review of the synthesis methods, characterization techniques and applications. *Renewable and Sustainable Energy Reviews*, 82, 1393–1414. <https://doi.org/10.1016/j.rser.2017.04.117>
- Guimarães, T., de Carvalho Teixeira, A. P., de Oliveira, A. F., & Lopes, R. P. (2020). Biochars obtained from arabica coffee husks by a pyrolysis process: characterization and application in Fe(II) removal in aqueous systems. *New Journal of Chemistry*, 44(8), 3310–3322. <https://doi.org/10.1039/C9NJ04144C>
- Illingworth, J. M., Rand, B., & Williams, P. T. (2022). Understanding the mechanism of two-step, pyrolysis-alkali chemical activation of fibrous biomass for the production of activated carbon fibre matting. *Fuel Processing Technology*, 235, 107348. <https://doi.org/10.1016/j.fuproc.2022.107348>
- López Nina, L. G., Valdez, S. O., Cabrera, S. O., Martínez, G. X., Surculento, R., Lara, R. M., Velasco, J. A., Torres, T. G., Tirado, N. S., & Zambrana, S. (2021). *Conversión de residuos domiciliarios de bioseguridad y residuos de poda en productos útiles: biochar y carbón activado*. Universidad Mayor de San Andrés.
- Marsh, H., & Rodríguez-Reinoso, F. (2006). *Activated carbon*. Elsevier.
- MELLIPIQ. (2025). *Activated Carbon Datasheets | Mellifiq*. <https://Mellifiq.Com/En/>. <https://mellifiq.com/en/activated-carbon-technical-datasheet/>
- Mochizuki, Y., Bud, J., Byambajav, E., & Tsubouchi, N. (2025). Pore properties and CO₂ adsorption performance of activated carbon prepared from various carbonaceous materials. *Carbon Resources Conversion*, 8(1). <https://doi.org/10.1016/j.crcon.2024.100237>
- Moussavi, G., Alahabadi, A., Yaghmaeian, K., & Eskandari, M. (2013). Preparation, characterization and adsorption potential of the NH₄Cl-induced activated carbon for the removal of amoxicillin antibiotic from water. *Chemical Engineering Journal*, 217, 119–128. <https://doi.org/10.1016/j.cej.2012.11.069>
- Newar, R., Sultana, N., & Baruah, A. (2026). Nanoarchitectonics of waste rice derived SiO₂@Activated carbon composite for high-performance adsorptive removal of CO₂ and cationic dyes. *Journal of Solid State Chemistry*, 354, 125733. <https://doi.org/10.1016/j.jssc.2025.125733>
- Nguyen, M. L., Ngo, H. L., Truong, B. N., & Nguyen, T. T. (2026). Soybean-residue-derived H₃PO₄-activated Carbon For High-Efficiency Adsorption of Hexavalent Chromium: Optimization, Characterization, and Adsorption Mechanisms. *Water, Air, & Soil Pollution*, 237(3), 174. <https://doi.org/10.1007/s11270-025-08828-9>
- Paradela, F., Pinto, F., Ramos, A. M., Gulyurtlu, I., & Cabrita, I. (2009). Study of the slow batch pyrolysis of mixtures of plastics, tyres and forestry biomass wastes. *Journal of Analytical and Applied Pyrolysis*, 85(1–2), 392–398. <https://doi.org/10.1016/j.jaap.2008.09.003>
- Rajadurai, B., & Chandradass, J. (2024). Mechanical, thermal, and morphological characterization of polylactic acid composites reinforced with coconut shell activated carbon. *Materials Research Express*, 11(11). <https://doi.org/10.1088/2053-1591/ad95e6>
- Ramirez, N., Sardella, F., Deiana, C., Schlosser, A., Müller, D., Kießling, P. A., Klepzig, L. F., & Bigall, N. C. (2020). Capacitive behavior of activated carbons obtained from coffee husk. *RSC Advances*, 10(62), 38097–38106. <https://doi.org/10.1039/d0ra06206e>
- Riyanto, C. A., Ampri, M. S., & Martono, Y. (2020). Synthesis and characterization of nano activated carbon from annatto peels (*Bixa orellana* L.) viewed from temperature activation and impregnation ratio of H₃PO₄. *EKSAKTA: Journal of Sciences and Data Analysis*, 1(1), 44–50.
- Şahin, Ö., Saka, C., Ceyhan, A. A., & Baytar, O. (2016). The pyrolysis process of biomass by two-stage chemical activation with different methodology and iodine adsorption. *Energy Sources, Part A: Recovery, Utilization, and Environmental Effects*, 38(12), 1756–1762. <https://doi.org/10.1080/15567036.2014.956195>
- Scheirs, J., & Kaminsky, W. (2006). Feedstock recycling and pyrolysis of waste plastics. In *Focus on Catalysts* (Vol. 2006, Number 9). [https://doi.org/10.1016/s1351-4180\(06\)71853-0](https://doi.org/10.1016/s1351-4180(06)71853-0)
- Serafin, J. (2017). Utilization of spent dregs for the production of activated carbon for CO₂ adsorption. *Polish Journal of Chemical Technology*, 19(2), 44–50. <https://doi.org/10.1515/pjct-2017-0026>
- Serafin, J., Antosik, A. K., Wilpiszewska, K., & Czech, Z. (2018). Preparation of Activated Carbon from the Biodegradable film for CO₂ Capture Applications. *Polish Journal of Chemical Technology*, 20(3), 75–80. <https://doi.org/10.2478/pjct-2018-0041>
- Serafin, J., & Dziejarski, B. (2023). Application of isotherms models and error functions in activated carbon CO₂ sorption processes. *Microporous and Mesoporous Materials*, 354, 112513. <https://doi.org/10.1016/j.micromeso.2023.112513>
- Shafeeyan, M. S., Daud, W. M. A. W., Shamiri, A., & Aghamohammadi, N. (2015). Modeling of Carbon Dioxide Adsorption onto Ammonia-Modified Activated Carbon: Kinetic Analysis and Breakthrough Behavior. *Energy & Fuels*, 29(10), 6565–6577. <https://doi.org/10.1021/acs.energyfuels.5b00653>
- Surculento Villalobos, R., Marín M., G. M., & Lopez N. L. (2023). Obtención de carbón activado a partir de mezclas de residuos de plásticos pet por activación con ácido fosfórico. *Revista Boliviana de Química*, 40(3). <https://doi.org/10.34098/2078-3949.40.3.3>